SC5344.7FR

2

11

RESEARCH ON FERROELECTRIC MATERIALS FOR MILLIMETER WAVE APPLICATION

Final Report
For Period August 5, 1981 through December 4, 1982

August 1983

DARPA Order No.:	4240
Program Code:	1D10
Name of Contractor:	Rockwell International Corporation
Effective Date of Contract:	August 5, 1981
Contract Expiration Date:	August 4, 1982
Amount of Contract Dollars:	$379,182
Contract Number:	F49620-81-C-0090
Principal Investigators:	Dr. R.R. Neurgaonkar (805) 498-4545, Ext. 109
	Dr. L.E. Cross Pennsylvania State University (814) 865-1181
	Dr. W.F. Hall (805) 498-4545 Ext. 189
	Dr. W.W. Ho (805) 498-4545 Ext. 194

Sponsored by

Defense Advanced Research Projects Agency (DoD)
DARPA Order No. 4240
Monitored by AFOSR/NE Under Contract No. F49620-81-C-0090

TABLE OF CONTENTS

		Page
1.0	SUMMARY	1
	1.1 Technical Problem	1
	1.2 General Methodology	2
	1.3 Technical Results	2
	1.4 Implications for Further Research	3
2.0	TUNGSTEN BRONZE COMPOSITIONS	4
	2.1 Single Crystal Growth of $Sr_{1-x}Ba_xNb_2O_6$ Compositions	5
	2.2 SBN:50 and SBN:60 Characterization	14
	2.3 The Tungsten Bronze $Pb_{1-2x}K_xM^{3+}_xNb_2O_6$ System	15
	2/4 PKLN/PKBN Characterization	17
3.0	HIGH FREQUENCY DIELECTRIC MEASUREMENTS	25
	3.1 Measurements of dn/dE	26
	3.2 Dielectric Studies	27
4.0	CONCLUSIONS	34
5.0	PUBLICATIONS AND PRESENTATIONS	35
	5.1 Publications	35
	5.2 Presentations	35
6.0	REFERENCES	36

LIST OF TABLES

Table		Page
2.1	Classification of Tungsten Bronze Family	5
2.2	Growth of SBN Single Crystals	9
2.3	Physical Properties of SBN	15
2.4	Physical Constants for Modified $PbNb_2O_6$	24
3.1	Variations of dn/dE with Frequency and Applied Voltage for SBN:50	27

UNCLASSIFIED

SECURITY CLASSIFICATION OF THIS PAGE (When Data Entered) Unclassified

REPORT DOCUMENTATION PAGE

READ INSTRUCTIONS BEFORE COMPLETING FORM

1. REPORT NUMBER: AFOSR-TR- 83-1299	2. GOVT ACCESSION NO.
3. RECIPIENT'S CATALOG NUMBER	
4. TITLE (and Subtitle): RESEARCH ON FERROELECTRIC MATERIALS FOR MILLIMETER WAVE APPLICATION	5. TYPE OF REPORT & PERIOD COVERED: FINAL REPORT 5 AUG 81 - 4 DEC 82
	6. PERFORMING ORG. REPORT NUMBER
7. AUTHOR(s): R. R. Neurganokar	8. CONTRACT OR GRANT NUMBER(s): F49620-81-C-0090
9. PERFORMING ORGANIZATION NAME AND ADDRESS: Rockwell international Corporation 1049 Camino Dos Rios P O Box 1085 Thousand Oaks, CA 91360	10. PROGRAM ELEMENT, PROJECT, TASK AREA & WORK UNIT NUMBERS: 61102F 2306/B2
11. CONTROLLING OFFICE NAME AND ADDRESS: Air Force Office of Scientific Research/NE Building #410 Bolling AFB, DC 20332	12. REPORT DATE: August 1983
	13. NUMBER OF PAGES: 39
14. MONITORING AGENCY NAME & ADDRESS(if different from Controlling Office)	15. SECURITY CLASS. (of this report): Unclassified
	15a. DECLASSIFICATION/DOWNGRADING SCHEDULE

16. DISTRIBUTION STATEMENT (of this Report)

Approved for public release; distribution unlimited.

17. DISTRIBUTION STATEMENT (of the abstract entered in Block 20, if different from Report)

18. SUPPLEMENTARY NOTES

19. KEY WORDS (Continue on reverse side if necessary and identify by block number)

Tungsten bronze compositions, Millimeter wave materials, Ferroelectric materials, Strontium barium niobate

20. ABSTRACT (Continue on reverse side if necessary and identify by block number)

OVER

DD FORM 1 JAN 73 1473 EDITION OF 1 NOV 65 IS OBSOLETE

Unclassified

SECURITY CLASSIFICATION OF THIS PAGE (When Data Entered)

20.

The largest and highest quality single crystals of the tungsten bronze family ferroelectric compositions of the strontium - barium niobate family reported to date were prepared by Czochralski growth techniques. Low frequency dielectric properties show low loss and high permittivity as expected. Accurate high frequency dielectric measurements for several compositions were made in a waveguide geometry from 30 to 100 GHz and the electric field sensitivity of the microwave refractive index, dn/dE, was evaluated by a modulation technique in the same waveguide geometry. Although high values of dn/dE were observed, an unexpectedly high dielective loss, which does not fit accepted models for dielectric properties, was observed. This fact, coupled with a high sample-to-sample variability, suggests a commonly occuring extrinsic factor such as growth defects or sample impurities as the key element limiting the use of these materials for phase control applications in millimeter wave radar systems. Similar dielectric measurements were made on a variety of ceramic ferroelectrics. In general the losses were substantially higher in these materials.

LIST OF TABLES

Table		Page
3.2	Dielectric Properties of Two SBN:60 Samples Before and After Poling	29
3.3	Dielectric Properties of Three Annealed SBN:60 Samples	30
3.4	Dielectric Properties of High Purity SBN:60 Samples	31
3.5	Summary of Measured Dielectric Properties of Single Crystal TiO_2	32
3.6	Dielectric Properties of Orthorhombic PKLN Samples	33

LIST OF FIGURES

Figure		Page
2.1	Phase boundary and Curie temperatures vs composition for $Sr_{1-x}Ba_xNb_2O_6$	7
2.2	SBN:50 single crystal grown along the (001) direction	10
2.3	SBN:60 single crystal grown along the (001) direction	11
2.4	Idealized form of SBN single crystals	12
2.5	Variation of lattice parameters for the $Pb_{1-2x}K_xLa_xNb_2O_6$ solid solution	18
2.6	Dielectric constant vs temperature of $Pb_{1-2x}K_xLa_xNb_2O_6$	19
2.7	Variation of the ferroelectric transition temperature for $Pb_{1-2x}K_xM_xNb_2O_6$, M = La or Bi	20
2.8	$Pb_{1-2x}K_xLa_xNb_2O_6$ dielectric properties as a function of sintering temperature	23

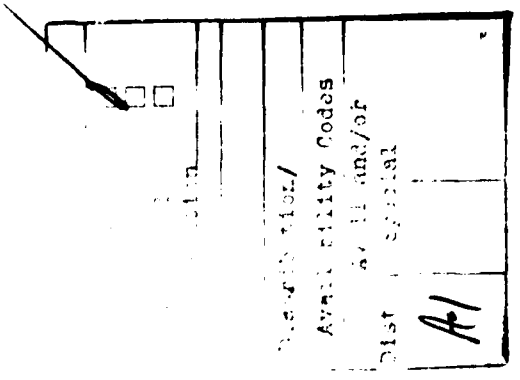

1.0 SUMMARY

This technical report presents the results of the final three months of a research program on ferroelectric materials for phase control applications in millimeter wave radar systems. Originally a one-year program, this effort was extended to fifteen months to take advantage of materials development activities in related programs. The major accomplishments in the current period include measurements of the electric field sensitivity of the microwave refractive index in strontium barium niobate single crystals, and development of growth techniques for $Sr_{0.5}Ba_{0.5}Nb_2O_6$ (SBN:50) single crystals of diameter exceeding 2 cm.

1.1 Technical Problem

On the basis of current models for ferroelectric materials, one predicts that certain ferroelectrics having a high dc permittivity $\varepsilon(o)$ should also show high sensitivity of their microwave refractive index, $n = \sqrt{\varepsilon(\omega)}$ to an applied electric field for microwave frequencies up to several hundred GHz. A low absorptive loss is also predicted over the same range of frequencies. However, the millimeter wave dielectric properties of these materials are largely unknown, and growth of the most promising ferroelectrics in single crystal form is generally difficult.

The present program was conceived on the basis of successful growth at Rockwell of one such ferroelectric, $Sr_{0.61}Ba_{0.39}Nb_2O_6$ (SBN:60), and measurement in this material of a substantial electric field sensitivity, dn/dE, of 10^{-6} meters/volt at 58 GHz.[1] With about an order of magnitude larger sensitivity, one can design microwave components operating at practical control voltages (under 200 volts) for phase shifting, modulation and switching. One attractive concept is a planar dielectric lens for electronically steering a millimeter wave radar beam, which could be used in high speed seeker applications.

The technical objective of the current study is to explore the range of dielectric properties (primarily dn/dE and dielectric loss) achievable within the SBN family. Other promising ferroelectrics are to be examined depending on availability.

1.2 General Methodology

There is an on-going program in development of growth techniques for tungsten-bronze materials at Rockwell, which provides the principal source for the $Sr_{1-x}Ba_xNb_2O_6$ ferroelectrics studied under the present contract. This program has produced the largest and highest quality single crystals reported to date of $Sr_{0.61}Ba_{0.39}Nb_2O_6$, the congruently melting composition.[2] Having these crystals available as seeds greatly facilitates the Czochralski growth of other SBN compositions and certain other tungsten bronzes. Also, through the ferroelectrics program at Penn State University, a wide variety of other materials have been made available for this study. These include ferroelectric and antiferroelectric ceramics, as well as single crystals, many of which have been well characterized by piezoelectric and low frequency dielectric measurement techniques.

Accurate high frequency dielectric measurements on the selected system have been carried out in a waveguide from 30 to 100 GHz.[3] Power reflection and transmission coefficients were determined on samples cut to fill the guide, and sample dielectric properties were fitted to these observations. The electric field sensitivity of the microwave refractive index, dn/dE, was evaluated by a modulation technique in the same waveguide geometry.

1.3 Technical Results

During the first six months of this program, millimeter wave measurements on SBN:60 single crystals revealed unexpected behavior which does not fit accepted models for the dielectric properties. Principally, a high level of dielectric loss was found in all samples, and relatively large decreases were noted in permittivity from the low frequency values. Since the envisioned phase control applications require much lower loss, the source of the observed high loss and its dependence on controllable factors has become our primary interest.

In the second six months, several SBN:60 single crystal samples grown from ultra-pure chemicals were characterized from 30 to 40 GHz, and from 90 to 100 GHz. Measurements of polar axis dielectric properties, both above and below

the Curie point, were made from 30-40 GHz. In addition, measurements on two ceramic systems, lead potassium lanthanum niobate (PKLN)[4] and barium strontium titanate (BST), were undertaken. These systems possess unusual low frequency dielectric properties which may provide viable alternatives for achieving phase control.

1.4 Implications for Further Research

All systems examined to date exhibit high dielectric loss at millimeter wavelengths, the minimum being tan $\delta_{11} \sim 0.03$ near 40 GHz for a high purity SBN:60 sample. The generality of this observation, when coupled with high sample-to-sample variability, suggests a commonly occurring extrinsic factor, such as growth defects, as the key element. How the frequency scale for polarization fluctuations is tied to such extrinsic influences remains to be explored. A systematic study of the influence of defect structure on microwave dielectric properties of ferroelectrics is probably the most appropriate next step.

2.0 TUNGSTEN BRONZE COMPOSITIONS

The goal of the present research program has been to investigate and develop new classes of ferroelectric materials for millimeter wave device applications. In seeking new materials that have excellent ferroelectric and dielectric properties with substantially low dielectric losses at millimeter wave frequencies, it is important to look for families that originate from high prototypic symmetry with possibilities for lower temperature ferroelectric-paraelectric phase transitions. For this reason, the tungsten bronze structural family is potentially important. The bronze compositions can be represented by general formulae $(A_1)_4(A_2)_2C_4B_{10}O_{30}$ and $(A_1)_4(A_2)_2B_{10}O_{30}$, in which A_1, A_2, C and B are 15-, 12-, 9-, and 6-fold coordinated sites in the structure. Because this family embraces some 100 or more known compounds and several solid solution systems, there is a good possibility for obtaining suitable compositions of the desired ferroelectric and and high frequency dielectric properties. This very large family of tungsten bronze materials offers a broad range of ferroelectric properties with the possibility of "fine tuning" the material response by composition manipulation, and hence is of major interest for potential millimeter wave device applications.

Based on our current work, the tungsten bronze family compositions, as summarized in Table 2.1, can be divided into two subgroups. This classification has mainly been developed on the basis of their unit cell dimensions, their crystal growth habits and physical properties which include, for example electro-optic, dielectric and piezoelectric coefficients. Compositions for both of these subgroups exhibit interesting, and sometimes contrasting properties. For this work the tetragonal tungsten bronze $Sr_{1-x}Ba_xNb_2O_6$ (SBN) system has been selected for millimeter wave study because of its excellent ferroelectric properties and extensive characterization. Single crystal growth of SBN by the Czochralski technique has been under development at Rockwell International for several years, and the growth of high quality, crack-free, large diameter single crystal material has been highly successful. This tungsten bronze system belongs to the class of smaller unit cell compositions, with the crystallographic c site vacant; hence it is referred to as an "unfilled" bronze structure.

Table 2.1

Classification of Tungsten Bronze Family

T.B. Compositions with Smaller Unit Cell Dimensions e.g., $Sr_{1-x}Ba_xNb_2O_6$ $Sr_2KNb_5O_{15}$	T.B. Compositions with Larger Unit Cell Dimensions e.g., $Ba_6Ti_2Nb_8O_{30}$, $Sr_2Ti_2Nb_8O_{30}$ $Ba_{2-x}Sr_xK_{1-y}Na_yNb_5O_{15}$, etc.
• Crystal Habit is Cylindrical with 24 Defined Facets	• Crystal Habit Square with 4 Defined Facets
• High Electro-Optic and Pyroelectric Effects	• High Electro-Optic Coefficient
• High Dielectric Constant	• Relatively Low Dielectric Constant
• High Piezoelectric d_{33} Coefficient but Low d_{15}	• High Piezoelectric d_{15} Coefficient but Low d_{33}
• Large Crystals with Excellent Quality are Available (2 - 3.0 cm in Diameter)	• Moderately Large Crystals are Available (~ 1 - 1.5 cm)

Another bronze system, $Pb_{1-2x}K_xM_x^{3+}Nb_2O_6$, where M = La or Bi, studied in this work is based on the unfilled orthorhombic structure of $PbNb_2O_6$. In this case the addition of $K^+ + M^{3+}$ ions not only stabilizes the structure by occupying the 15- and 12-fold coordinated sites, but also enhances the dielectric and piezoelectric properties of this solid solution system. Furthermore, in the orthorhombic phase this system has a spontaneous polarization with components along two crystallographic directions, namely the c- and b-axes, and this should give rise to interesting behavior in the millimeter wave cross-axis dielectric sensitivity to an applied electric field.

A discussion of the growth of these bronze compositions and their structural and ferroelectric properties is given in the following sections.

2.1 Single Crystal Growth of $Sr_{1-x}Ba_xNb_2O_6$ Compositions

Considerable effort has been made to grow and characterize $Sr_{1-x}Ba_xNb_2O_6$, x = 0.4 and 0.5, solid solution crystals grown by the Czochralski

technique.[2,5] We have now demonstrated the ability to grow large diameter (2 to 3 cm) SBN:60 and SBN:50 single crystals which show good electrical, mechanical and optical quality for potential use in a wide variety of applications. Although the end members $SrNb_2O_6$ and $BaNb_2O_6$ do not belong to the tungsten-bronze structural family, the solid solution $Sr_{1-x}Ba_xNb_2O_6$ crystallizes in the tetragonal tungsten bronze structure for $0.25 < x < 0.75$.[6]

Figure 2.1 shows the limit of solid solubility range for the three different phases, e.g., $SrNb_2O_6$, $BaNb_2O_6$ and $Sr_{1-x}Ba_xNb_2O_6$, and the variation of the ferroelectric phase transition temperature for the tungsten bronze solid solution. This tungsten bronze solid solution has been shown to be very useful for several device applications since it exhibits the largest electro-optic[7] and pyroelectric coefficients of any well behaved material.[8] According to our current work, this solid solution possesses temperature compensated orientations[6] and should also be useful for millimeter wave applications.

Work by Megumi et al[9] indicates that the composition $Sr_{0.60}Ba_{0.40}Nb_2O_6$ (SBN:60) is the only congruently melting composition of the entire series. The Czochralski growth technique has already been established for SBN:60, and crystals as large as one-inch diameter have been developed. This technique has been applied to other compositions within this solid solution. Although the composition $Sr_{0.50}Ba_{0.50}Nb_2O_6$ is not congruently melting, it exhibits interesting ferroelectric and optical properties; it was selected in the present work to compare its high frequency dielectric properties to those of SBN:60 and thereby obtain information on the range of properties available in the SBN system.

Initially, SBN:50 crystals were pulled using SBN:60 crystals as seeds, and this proved successful in obtaining reasonably large seed material for subsequent Czochralski growths of this composition. Several fracture-free and reasonably good quality single crystals of SBN:50 and SBN:60 have now been successfully grown, with crystal diameters in the range of 1 to 3 cm. These crystals were pulled along the crystallographic c-axis (001), and although growths along other orientations such as (100) and (110) have been performed, it

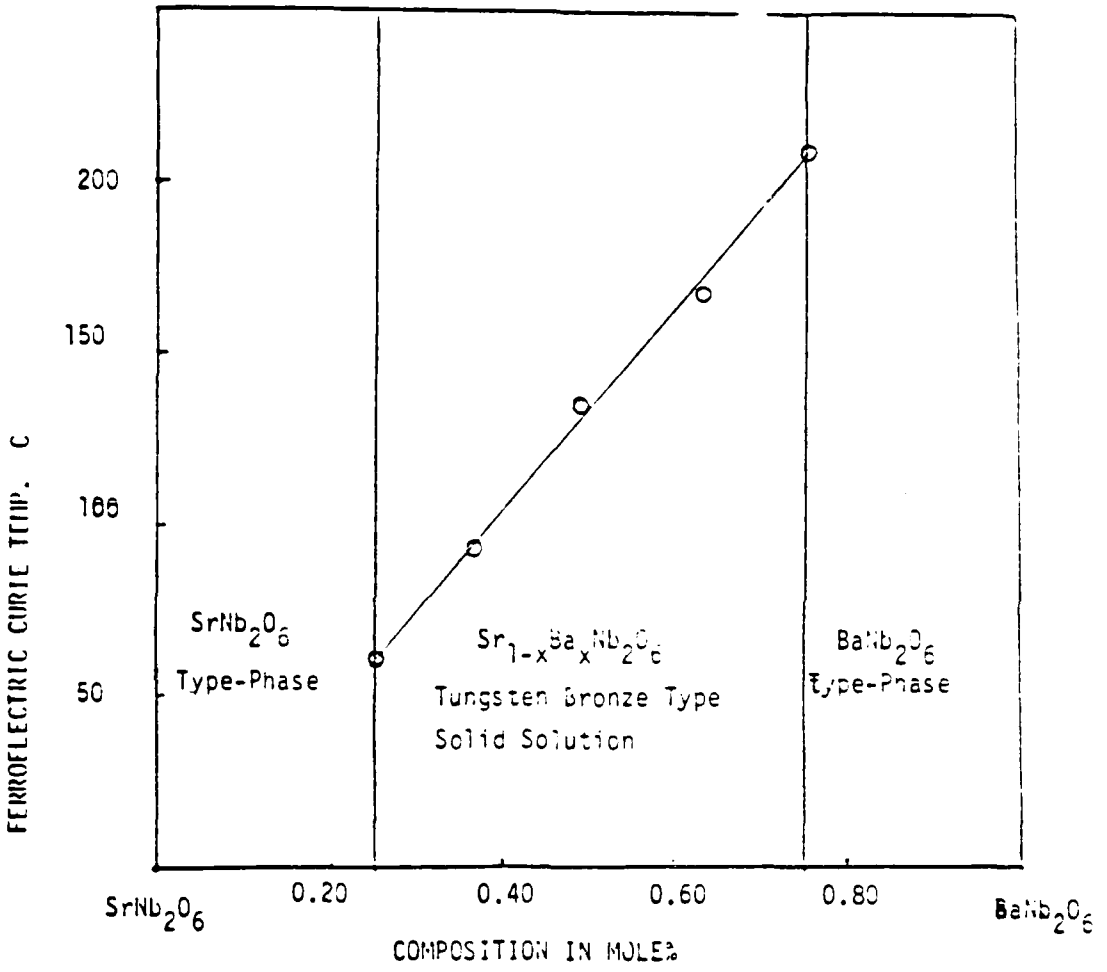

Fig. 2.1 Phase boundary and Curie temperatures vs composition for $Sr_{1-x}Ba_xNb_2O_6$.

is difficult to obtain reasonable size, good quality crystals in these other growth directions. A summary of the growth conditions for several SBN crystals is given in Table 2.2. The use of an automatic diameter control (ADC) system in our new Czochralski puller has significantly improved the general quality of the crystals grown, and is now in regular use.

Figures 2.2 and 2.3 show typical c-axis growths for SBN:50 and SBN:60, respectively. These crystals are usually well faceted, which is unusual for Czochralski-grown crystals. X-ray diffraction studies show that the crystal habits are based on 24 faces of four prisms: (110), (120), (100) and (130). These observations are in excellent agreement with results reported by Dudnik et al[10] for the $Sr_{1-x}Ba_xNb_2O_6$ solid solution single crystals. The idealized form of the crystal is shown in Fig. 2.4. The crystals are pale yellow to yellow as grown depending on the crystal diameter. Since the ferroelectric phase transition temperatures for these compositions are low, in the range of 120°C or less, the crystals were cooled with great care to room temperature in order to minimize the potential for cracking.

Since the SBN solid solution system exists over such a wide compositional range (Fig. 2.1), bulk single crystal growth by the Czochralski technique can be very difficult. The main problem associated with this technique can be summarized as crystal diameter instability during growth and thermal cracking. Inhomogeneity along the growth direction and core causes strain central to the growth axis, accounts for the presence of striations in the crystals, and may also affect dielectric losses at both low and high frequencies.

The problem associated with coring has been largely eliminated in SBN:60 crystals by pulling the crystals at a composition as close to the congruent melt as possible. However, since SBN:50 is not a congruent melting composition, the growth of defect-free crystals in this case is much more difficult, and therefore SBN:50 crystal diameters have been generally confined to 1 cm or less. The presence of significant optical striations and high dielectric losses at millimeter wave frequencies ($\tan \delta > 0.1$) in early growths of these compositions are believed to be due to several experimental factors. Most authors concerned with the growth of SBN report the existence of striae

Table 2.2

Growth of SBN Single Crystals

Exp No.	Composition (001 Growth)	Pull Rate	Rotation Rate (rpm)	Boule Weight (gms)	Growth Temperature (°C)	Color	Remarks
126	SBN:60	6 mm/hr	0 - 20	10	1510	Colorless	7 mm in diameter 3 cm long
127	SBN:60	5 - 6 mm/hr	0 - 10	58	1510	Pale Yellow	ADC - uncracked
133	SBN:60	5 - 6 mm/hr	5	20	1510	Pale Yellow	ADC - uncracked
134	SBN:60	6 - 8 mm/hr	10	35	1510	Pale Yellow	ADC - uncracked
142	SBN:60	2 - 10 mm/hr	0 - 30	10	1510	Almost Colorless	Uncracked
143	SBN:60	3 - 15 mm/hr	0 - 10	9	1510	Almost Colorless	Cracked on cutting
144	SBN:60	8 - 12 mm/hr	5 - 8	21	1510	Pale Yellow	ADC - uncracked.
145	SBN:60	8 - 12 mm/hr	5 - 8	18	1510	Pale Yellow	ADC - uncracked
147	SBN:60	8 - 15 mm/hr	3 - 9	24	1510	Pale Yellow	Half crystal cracked
123	SBN:50	7 mm/hr	10	16	1520	Pale Yellow	Cracked on cutting
124	SBN:50	8 mm/hr	8	20	1520	Pale Yellow	Cracked severely
125	SBN:50	8 mm/hr	8	30	1520	Pale Yellow	Uncracked
132	SBN:50	8 mm/hr	10	28	1520	Pale Yellow	Re-annealed at 1200°C, uncracked
146	SBN:50	6 mm/hr	5	27	1520	Pale Yellow	Re-annealed, uncracked

SBN:60 - $Sr_{0.6}Ba_{0.4}Nb_2O_6$.

SBN:50 - $Sr_{0.5}Ba_{0.5}Nb_2O_6$

ADC - Automatic diameter control.

SC83-22629

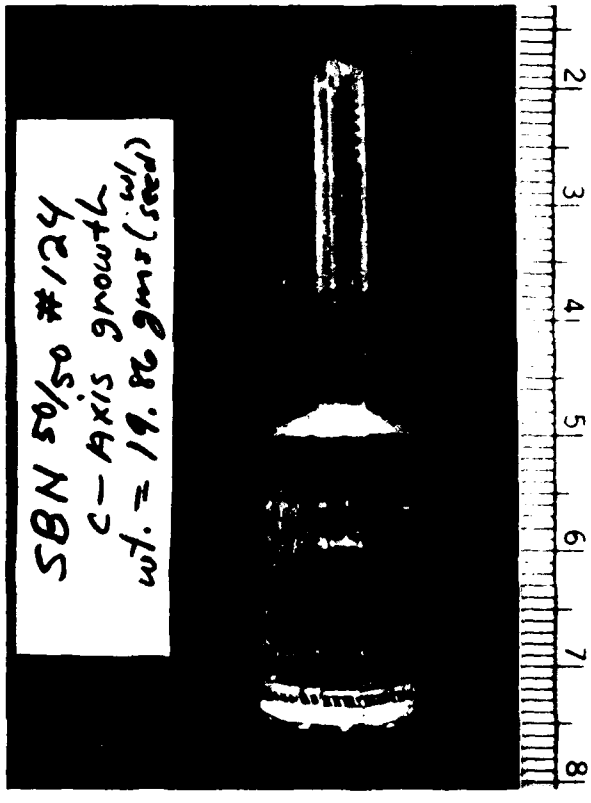

Fig. 2.2 SBN:50 single crystal grown along the (001) direction.

SC83-22628

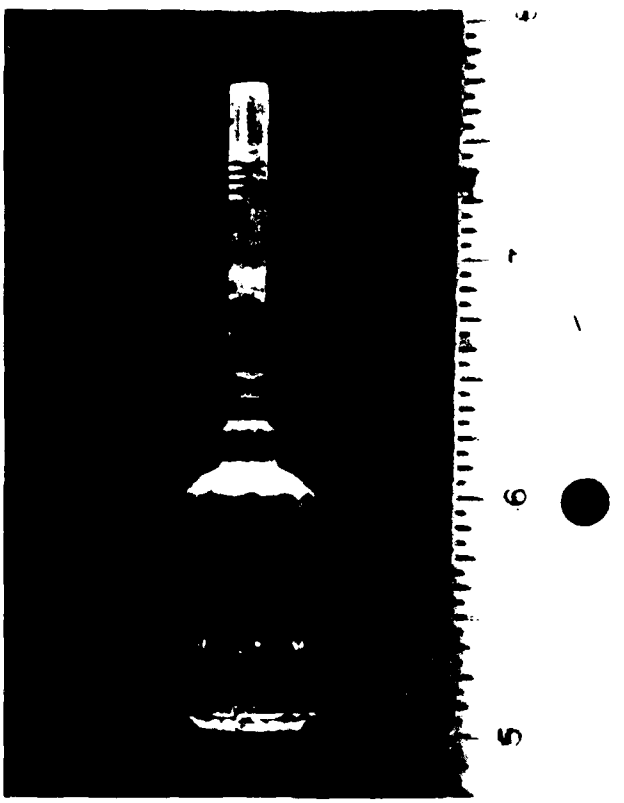

Fig. 2.3 SBN:60 single crystal grown along the (001) direction.

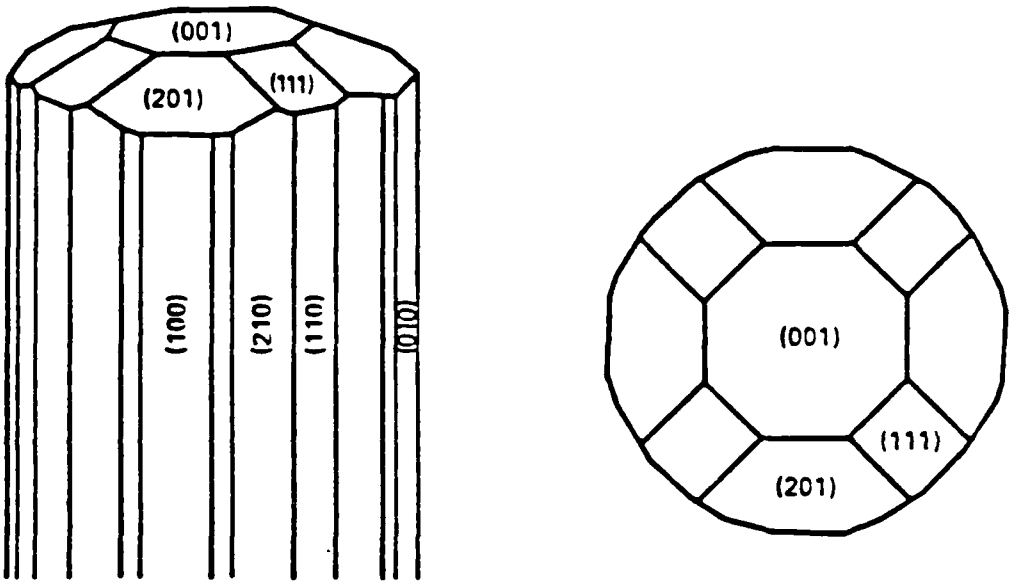

Fig. 2.4 Idealized form of SBN single crystals.

(or refractive index variations) in these crystals. The striae are generally attributed to variations in the growth temperature causing variations in the composition, in particular the Sr/Ba ratio. Besides this problem, we suspect that there are some other problems which are responsible for introducing defects in SBN single crystals. They are as follows:

a. Reduction of Nb^{5+} to Nb^{4+} at the growth temperature (if oxygen pressure is low). Nb^{4+} acts as an impurity.

b. Presence of impurities, e.g., Ca^{2+} and Fe^{3+}, in the starting materials. Initially reagent grade chemicals were used in this work.

c. Temperature fluctuation in our old pulling unit (± 3 - 5°C) responsible for excessive temperature instability.

As mentioned previously, a new Czochralski growth unit with automatic diameter control (ADC) has been installed and has been in service for the past six months. The system has been modified to provide further improvement in temperature stability (± 2°C). If necessary, other modifications will be made in this system to provide even better temperature stability in future growths.

We recently analyzed several crystals which were grown using analar grade as well as higher purity chemicals, and found that striations are definitely connected to a nonuniform distribution of impurity ions such as Ca^{2+}, Fe^{3+}, Nb^{4+} and Ir^{4+} (if an Ir crucible is used). These impurities were found to be on the order of 80 ppm or higher in concentration (analar grade chemicals), and greatly affect crystal quality and coloration. For example, Fe^{3+}-containing crystals are deep yellow in color, while Nb^{4+}- and Ir^{4+}-containing crystals are purple to coal black in color, depending on the concentration of impurity ions. The inclusion of Nb^{4+}, which results from a reduction of Nb^{5+}, has been eliminated to a large extent by employing an oxygen pressure of two atmospheres or more. Since the concentration of Fe^{3+} and Ca^{2+} is significantly lower in higher purity starting materials, striations are substantially reduced, but do

not completely disappear. Based on these observations, it is clear that future experiments can be redesigned by either improving the temperature stability during growth and/or by use of still higher purity chemicals. At this stage, it appears that temperature stability is now a more significant factor and plans are underway to further modify the thermal gradient in and above the crucible. We believe that if we can succeed in controlling temperature stability to 0.5 - 1.0°C or better, it may be possible to significantly improve SBN crystal quality and further enhance its potential for use in a number of device areas.

2.2 SBN:50 and SBN:60 Characterization

Powder x-ray diffraction measurements for $Sr_{1-x}Ba_xNb_2O_6$, x = 0.50, 0.40 show a room temperature tungsten bronze tetragonal structure, and according to the structural refinements by Jamieson et al[11] for $Sr_{0.75}Ba_{0.25}Nb_2O_6$ crystals, this solid solution system belongs to the point group 4 mm. Lattice parameter measurements from x-ray data on ceramic and single crystal samples give values of a = 12.482A and c = 3.953A for SBN:50, and a = 12.475A and c = 3.941A for SBN:60, in good agreement with the published results of Jamieson.[11]

SBN:50 and SBN:60 compositions have been extensively characterized for their low frequency dielectric, piezoelectric and optical properties. Measurements were made using deposited gold or platinum contacts on the various sample orientations. Crystal poling along the c-axis was achieved by field-cooling from slightly above the Curie temperature with an applied field in the range of 6 - 7.5 kV/cm. A summary of these results is given in Table 2.3. These room temperature data are excellent, making both SBN:50 and SBN:60 of significant interest for a number of ferroelectric device applications.

Table 2.3
Physical Properties of SBN

Property	$Sr_{0.50}Ba_{0.50}Nb_2O_6$	$Sr_{0.60}Ba_{0.40}Nb_2O_6$
Curie Temp (°C)	125	72
Dielectric Constant K_{33}, at 23°C	500	880
Electromechanical Coupling		
k_{15}	-	0.13
k_{31}	0.137	0.14
k_{33}	0.48	0.47
Piezoelectric Strain Coeff. (1×10^{-12} C/N)		
d_{15}	24	31
d_{33}	100	130
Electro-Optic Coeff. r_{33} (m/V)	130×10^{-12}	420×10^{-12}

2.3 The Tungsten Bronze $Pb_{1-2x}K_xM^{3+}_xNb_2O_6$ System

The $Pb_{1-2}K_xM^{3+}_xNb_2O_6$ system is based on the orthorhombic tungsten-bronze $PbNb_2O_6$ phase, which was the first oxide ferroelectric ever discovered that was not a perovskite.[12,13] $PbNb_2O_6$ has been used commercially as a piezoelectric ceramic transducer. Its outstanding features are its ability to withstand exposure to temperatures approaching its Curie point (560°C) without severe depoling, its large d_{33}/d_{31} ratio, and its extremely low mechanical Q. Above the Curie point, the structure is tetragonal with lattice constants, a = 12.56 and c = 3.925Å, space group P4/mbm, isostructural with potassium tungsten bronze. Below the Curie point, there is slight orthorhombic distortion, quadrupling the cell size, with lattice constants becoming a = 17.63, b = 17.93 and c = 7.736Å, space group Cmm2.

Although the Curie temperature was much higher than that of any known ferroelectric, the material did not find immediate application because of the difficulty in preparing good nonporous ceramics and the associated problem of poling them. By analogy with previous work on barium titanate and other ferroelectric hosts, the effect of replacing part of Pb^{2+} by other divalent and trivalent ions, or Nb^{5+} by tetravalent or hexavalent ions was studied,[14-24] with the objective of improving the sintering and general ferroelectric properties of the ceramic. It was observed that the Curie temperature decreased, and although this would be an disadvantage, this made it possible to pole the material more effectively and successfully enhance the dielectric and piezoelectric properties. The systems $Pb_{1-2x}K_xM^{3+}_xNb_2O_6$, M = La or Bi, and $Pb_{1-x}Ba_xNb_2O_6$ are typical examples of such substitutions. Their dielectric and piezoelectric properties are excellent and they are promising candidates for high frequency dielectric studies.

Since $Pb_{1-2x}K_xM^{3+}_xNb_2O_6$ is a relatively new tungsten bronze system, and furthermore, since single crystal growth of lead-containing oxides is very difficult due to lead volatilization at the melt temperature, the work on this system for this program has been confined to sintered ceramic samples. PbO, K_2CO_3 (Baker Analyzed Grade), Bi_2O_3 (Fisher Scientific Co.), La_2O_3 (American Potach and Chem. Corp.), and Nb_2O_5 (Atomergic Co.) were used as the starting materials. The ceramic specimens were prepared by the conventional technique of milling, prefiring, crushing, pressing and firing. The specimens were prepared in the form of disks 1.3 cm in diameter and 0.3 cm thick. The final sintering was for 2 - 3 hr, and the temperature, which depended on composition, was between 1250° - 1300°C.

The work on $K_{0.5}La_{0.5}Nb_2O_6$ by Soboleva et al.[25] and our work on $K_{0.5}Bi_{0.5}Nb_2O_6$ show that these two phases crystallize in the tetragonal crystal symmetry and are isostructural with the high temperature tetragonal modification of $PbTa_2O_6$. At room temperature, the ferroelectric $PbTa_2O_6$ phase has an orthorhombic symmetry and is isostructural with the tungsten bronze $PbNb_2O_6$ phase. This suggests that all the systems considered in this work are structurally related and should form a continuous solid solution in the pseudo-binary systems $PbNb_2O_6$-$K_{0.5}La_{0.5}Nb_2O_6$ and $PbNb_2O_6$-$K_{0.5}Bi_{0.5}Nb_2O_6$. The results of x-ray dif-

fraction powder work are in good agreement, and a complete solid solution has been identified in both of the systems. Three structural related phases, namely, the orthorhombic and the tetreagonal tungsten bronze type phases and the tetragonal $K_{0.5}La_{0.5}Nb_2O_6$, have been established for the $Pb_{1-2x}K_xM^{3+}_xNb_2O_6$, M = La or Bi, solid solution system.

The results of x-ray measurements at room temperature show a homogeneity range of the orthorhombic tungsten bronze phase to x = 0.47, while the tetragonal tungsten bronze phase is present in the composition range $0.48 > x > 0.85$. At the other end, the crystalline solid solubility of $PbNb_2O_6$ in the $K_{0.5}M^{3+}_{0.5}Nb_2O_6$ phase is limited and is estimated to be in the composition range $0.86 > x > 1.0$. At composition x = 0.47, both the orthorhombic and tetragonal tungsten bronze phases coexist. This type of morphotropic condition has also been reported on the $Pb_{1-x}Ba_xNb_2O_6$ system.[14,21] The variation of lattice parameters as a function of composition for the system $Pb_{1-2x}K_xLa_xNb_2O_6$ is shown in Fig. 2.5. The a and c parameters increase only slightly, while the b parameter decreases considerably with increasing concentration of $K_{0.5}M^{3+}_{0.5}Nb_2O_6$ in the $PbNb_2O_6$ phase. The decrease in the b parameter is substantial compared to the a parameter, so that the ratio b/a becomes close to unity for values $x < 0.50$.

2.4 PKLN/PKBN Characterization

A typical plot of the low frequency (10 kHz) dielectric constant vs temperature is given in Fig. 2.6 for a few compositions in the $Pb_{1-2x}K_xLa_xNb_2O_6$ system. It can be seen that the dielectric constant decreases and broadens whereas the room temperature dielectric constant increases with increasing K^+ and La^{3+} or Bi^{3+} up to x = 0.40. Furthermore, the ferroelectric phase transition temperature T_c is shifted towards a lower temperature with increasing amounts of $K_{0.5}La_{0.5}Nb_2O_6$ in $PbNb_2O_6$. T_c for the pure $PbNb_2O_6$ has been recorded at 560°C, and this temperature drops with the addition of K^+ and La^{3+} or Bi^{3+} in both the orthorhombic and the tetragonal tungsten bronze phases. By using this peak position, the transition temperature for each system has been determined. Figure 2.7 shows the variation of the Curie temperature of T_c as a function of composition for the $Pb_{1-2x}K_xLa_xNb_2O_6$ and $Pb_{1-2x}K_xBi_xNb_2O_6$ systems. Variation

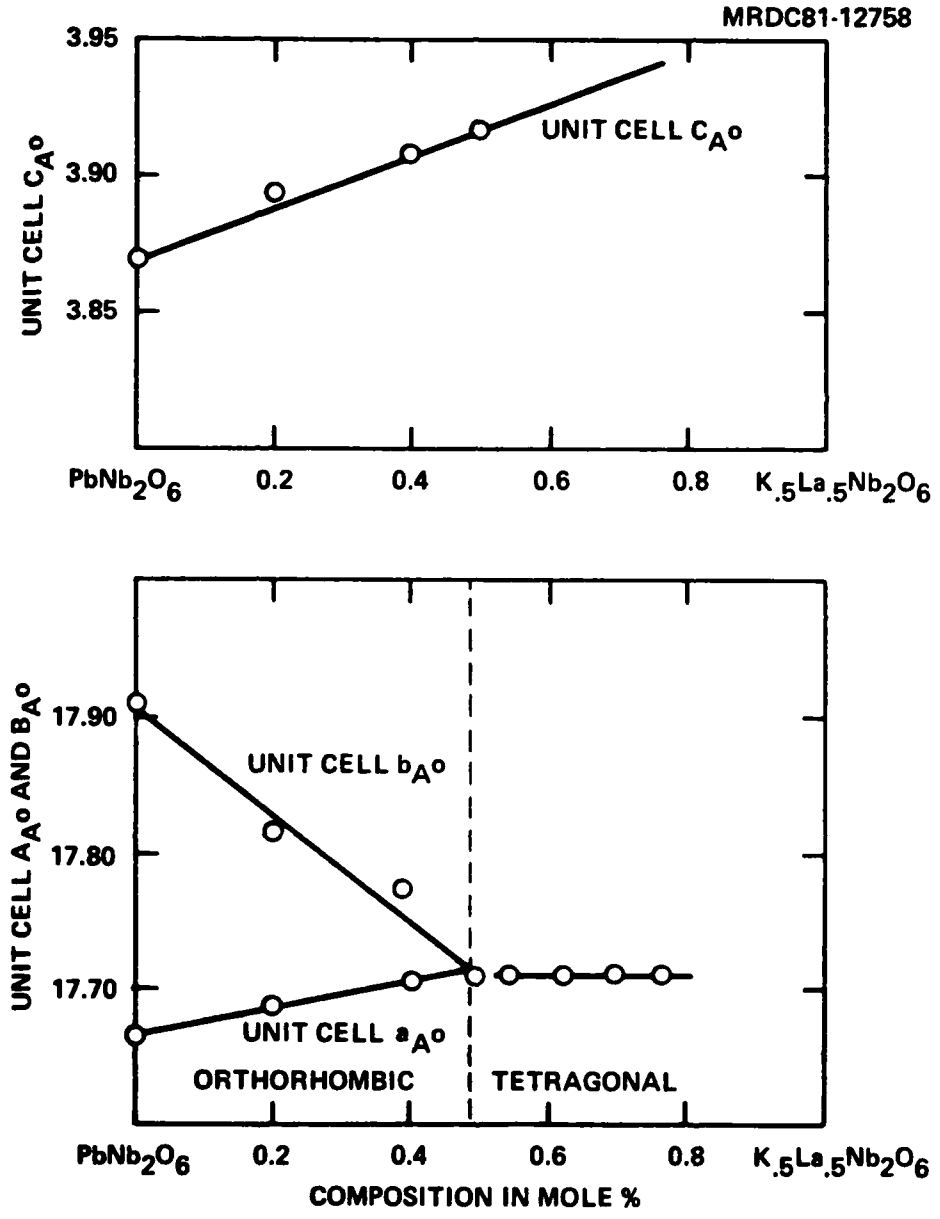

Fig. 2.5 Variation of lattice parameters for the $Pb_{1-2x}K_xLa_xNb_2O_6$ solid solution.

SC82-17598

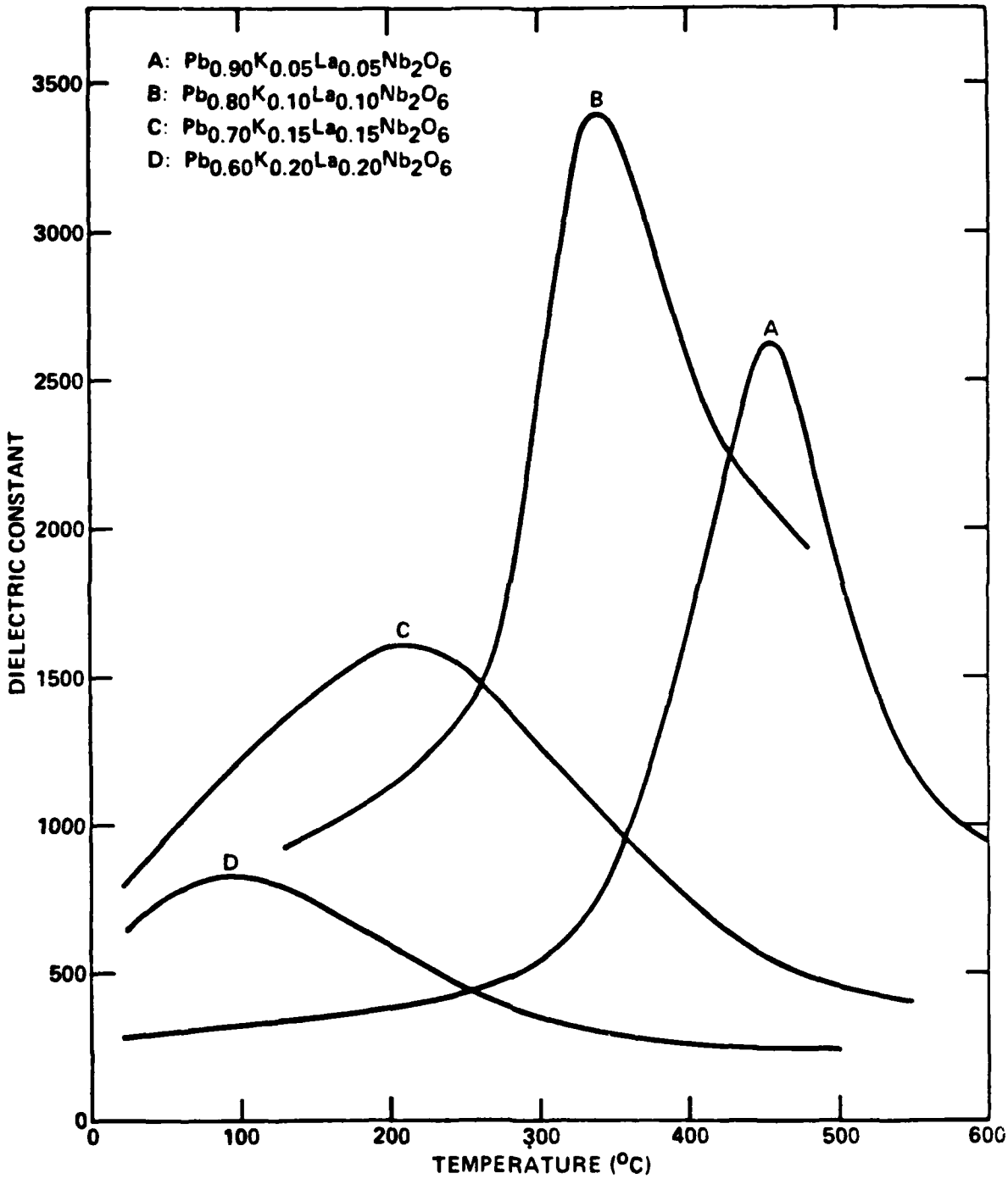

Fig. 2.6 Dielectric constant vs temperature of $Pb_{1-2x}K_xLa_xNb_2O_6$.

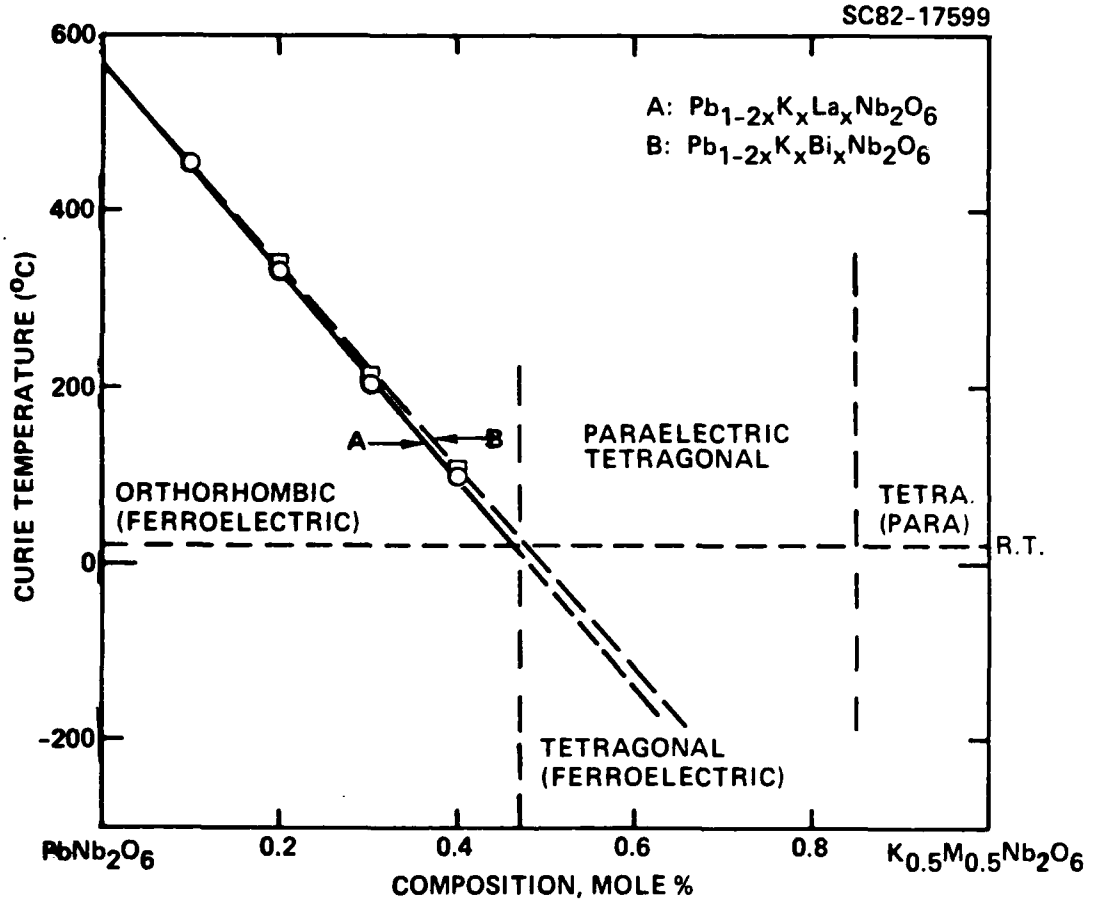

Fig. 2.7 Variation of the ferroelectric transition temperature for $Pb_{1-2x}K_xM_xNb_2O_6$, M = La or Bi.

of T_c with composition is linear in both systems and is approximately of the same order. Lowering of T_c has also been reported for several other systems based on $PbNb_2O_6$ solid solutions.[15,18-23]

The effect of a variety of different substituent ions, such as Ba^{2+}, Sr^{2+}, Ca^{2+}, Cd^{2+} and Bi^{3+} for Pb in the $PbNb_2O_6$ phase, has been studied and reported in literature.[14-24] Except for Ba^{2+}, all other ions are smaller than Pb^{2+}, and their addition did not alter the orthorhombic crystal symmetry. However, in the case of the $Pb_{1-x}Ba_xNb_2O_6$ solid solution system, the substitution of Ba^{2+} (1.50A) for Pb^{2+} (1.32A) first decreases the orthorhombic distortion, and then induces a tetragonal structure with the polar axis along the c rather than along the b axis. Further, the interesting feature in this system is that T_c first decreases in the orthorhombic tungsten bronze phase and then increases in the tetragonal tungsten bronze phase. This is the unique case in the $PbNb_2O_6$ based solid solutions; also, since the average ionic size of K^+ + La^{3+} (1.355A) and K^+ + Bi^{3+} (1.34A) is bigger than Pb^{2+}, and since both systems, $Pb_{1-2x}K_xM_x^{3+}Nb_2O_6$, M = La or Bi, and $Pb_{1-x}Ba_xNb_2O_6$, are structurally similar, it was expected that the addition of K^+ with La^{3+} or Bi^{3+} would produce similar results, i.e., first a decrease and then an increase in T_c.

However, the results of this work (Fig. 2.7) indicate that a continuously decreasing Curie temperature occurs with increasing amounts of K^+ + La^{3+} or K^+ + Bi^{3+} in both the orthorhomic and tetragonal tunsten substitutional bronze phases, indicating that T_c is not only controlled by the size of substituent ions, but its location in the structure is equally important. Since the coordination of Pb^{2+} is 15- and 12-fold in the tungsten bronze structure, there exists three possibilities for each ion in this structure, namely in the 15 or 12, or in both sites. Neither the work reported in the literature[14-20] nor the results of this investigation are sufficient to establish the site preference or their distirbution over the two crystallographic sites. Further work in this direction is of significant interest in order to establish the site preferences for differnt ions and their influence over the behavior of the Curie temperature and the ferroelectric and millimeter wave dielectric properties.

Figure 2.8 shows the variation of the low frequency dielectric constant (at T_c and at room temperature) and the room temperature dielectric losses as a function of the sintering temperature for the $Pb_{0.8}K_{0.1}La_{0.1}Nb_2O_6$ composition. Data for other compositions are similar to that shown in Fig. 2.8. In general, the sintering temperature was held below 1290°C to avoid softening of the disks; soak time was 2 - 3 hours, with no significant improvement in the dielectric properties with longer times.

Table 2.4 summarizes the physical constants for the $Pb_{1-2x}K_xLa_xNb_2O_6$ (PKLN) and $Pb_{1-2x}K_xBi_xNb_2O_6$ (PKBN) systems. As can be seen from these data, the dielectric constant has increases significantly with the addition of K^+ and La^{3+} or Bi^{3+} in the orthorhombic tungsten bronze phase with the compositions $Pb_{0.8}K_{0.1}La_{0.1}Nb_2O_6$ (PKLN 80/20) and $Pb_{0.7}K_{0.15}Bi_{0.15}Nb_2O_6$ (PKBN 70/30) exhibiting the optimum dielectric constant for each system. The piezoelectric strain coefficient (d_{33}) measurements on various samples were performed using the Berlincourt d_{33}- meter and the results of this study indicate that the composition $Pb_{0.8}K_{0.1}La_{0.1}Nb_2O_6$ again shows the optimum d_{33} coefficient for these systems. We believe these values may increase substantially if the poling is achieved at higher temperatures. In the present case, poling was accomplished in a silicon oil bath at approximately 150°C, which is a very low temperature compared to the respective Curie temperatures. It is anticipated that by improving the poling technique for these ceramic samples it will be possible to better establish the d_{33} coefficient. In any case, the present piezoelectric strain coefficient value obtained for the $Pb_{0.8}K_{0.1}La_{0.1}Nb_2O_6$ sample is much higher than that reported for the $PbNb_2O_6$ crystal, indicating that these compositions can find use for piezoelectric transducer and high frequency dielectric applications. However, the results for the $Pb_{1-2x}K_xBi_xNb_2O_6$ compositions, although quite good, are not as good as those for the best of the $Pb_{1-2x}K_xLa_xNb_2O_6$ compositions. Furthermore, many of the PKBN samples proved to be difficult to pole; hence, for this study our work has focussed on compositions from the $Pb_{1-2x}K_xLa_xNb_2O_6$ system for millimeter wave dielectric characterization.

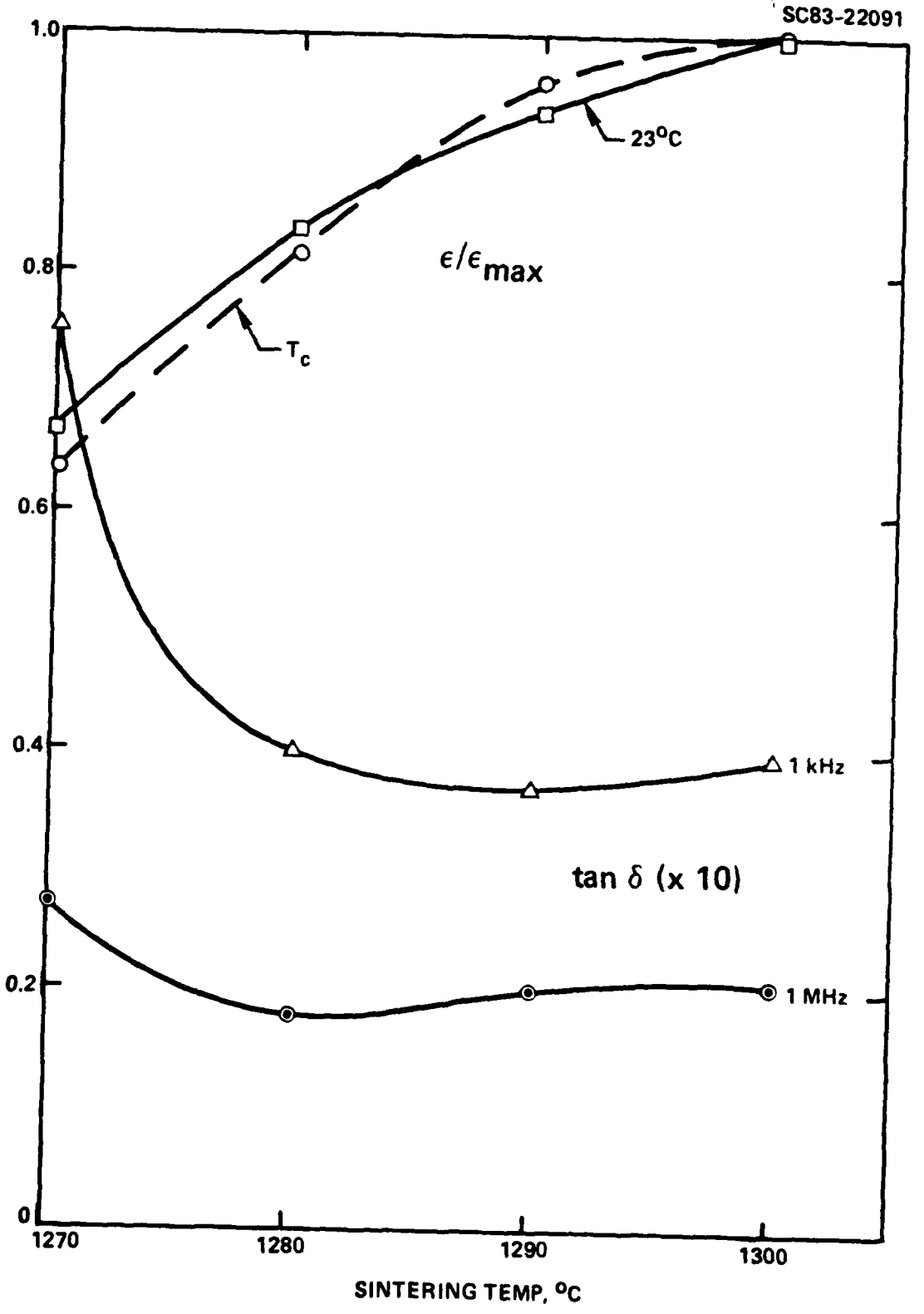

Fig. 2.8 $Pb_{1-2x}K_xLa_xNb_2O_6$ dielectric properties as a function of sintering temperature.

Table 2.4

Physical Constants for Modified $PbNb_2O_6$

Composition*	Curie Temperature T_c, °C	Dielectric Constant, K R.T.	Dielectric Constant, K T_c	Piezoelectric Strain Coeff., d_{33} c/n
$PbNb_2O_6$	560			100 10^{-12}
$Pb_{0.90}K_{0.05}La_{0.05}Nb_2O_6$	455	288	2610	---
$Pb_{0.80}K_{0.10}La_{0.10}Nb_2O_6$	339	720	3390	130 10^{-12}
$Pb_{0.70}K_{0.15}La_{0.15}Nb_2O_6$	201	790	1600	106 10^{-12}
$Pb_{0.60}K_{0.20}La_{0.20}Nb_2O_6$	98	650	830	---
$Pb_{0.80}K_{0.10}Bi_{0.10}Nb_2O_6$	342	280	2310	30 10^{-12}
$Pb_{0.70}K_{0.15}Bi_{0.15}Nb_2O_6$	211	750	2840	35 10^{-12}
$Pb_{0.60}K_{0.20}Bi_{0.20}Nb_2O_6$	105	1390	2380	---

*All compositions are orthorhombic.

3.0 HIGH FREQUENCY DIELECTRIC MEASUREMENTS

The primary objective of this contract effort has been to determine the feasibility of using the electric-field sensitivity of the microwave refractive index in available ferroelectrics as a means to control the phase of a transmitted millimeter wave radar beam. Using SBN:60 crystals grown in this laboratory, we had observed sensitivities dn/dE of the order of 10^{-6} meters/volt.[1] For the beam-steering application we envisioned, this sensitivity would require AC voltages around 2000 volts; an improvement to 10^{-5} meters/volt or higher was deemed necessary for implementation with currently avialable solid-state technology. Within the SBN family order-of-magnitude variations are observed in the electro-optic coefficients and other related properties, so it is reasonable to expect that dn/dE may attain much higher values in some of these materials. For more conventional waveguide phase shifters the measured sensitivity was already high enough.

A serious and unexpected limiting factor for all applications was discovered early in the contract effort: millimeter wave losses in the available ferroelectrics typically exceeded 20 dB per millimeter. To use such a material in the beam-steering application, an unrealistically thin phase-shifting layer, less than 50 microns, would be required in order to hold transmission losses to tolerable levels. The phase shifting electric field in such a layer would reach tens of kilovolts per centimeter, large enough to depole the film and destroy the basic effect.

The material factors which cause these large losses are not yet known. Based purely upon extrapolation from the low freuqency dielectric properties, one predicts losses in the neighborhood of 1 - 2 dB per millimeter until frequencies of several hundred gigaherz or temperatures a few degrees below the ferroelectric-paraelectric transition temperature are reached. We have investigated impurites, compositional fluctuations, and growth defects as possible sources for the observed high loss. However, as of this writing, no definite trends have been identified. Under separate contract with the Office of Naval Research, we are continuing to explore this phenomenon as part of a general study of millimeter wave properties of high dielectric constant materials.

For this final report, we have carried out measurements of dn/dE in SBN:60 and SBN:50 at frequencies between 30 and 40 GHz. Although the problem of high loss at present prevents attainment of the original goal, it is worthwhile to confirm our earlier measurements, and to establish the trend of values for dn/dE within the SBN solid solution system.

3.1 Measurements of dn/dE

The method of measurement is a straightforward application of transmission modulation similar to that described by Boyd et al.( ) In this technique, a properly oriented and poled sample in waveguide is subjected to a transverse low-frequency electric field, and the resulting modulation in transmitted power is synchronously detected.

Results of these measurements for SBN:60 are typified by the linear response illustrated in Fig. 3.1. In this figure, the left-hand axis compares the power variation in the modulated signal to the transmitted power in the absence of an applied field, while the right hand axis displays the change in permittivity required to produce the observed modulation. Sample thickness in this case was 1.12 millimeters. From the variation of permittivity with applied field, one calculates a value for the c-axis sensitivity dn_{33}/dE_3 of (5.83 ± 0.14) × 10^{-7} meters/Volt at 33 GHz. This is about a factor of two smaller than the value obtained in our earlier work at 58 GHz. The equivalent electro-optic coefficient $r_{33} = 2\ n^{-3}\ dn/dE$ in this sample is 3.8 × 10^{-10} meters/Volt. The frequency dependence of dn/dE for this sample was not large, but showed an increasing trend from 30 to 35 GHz, reaching values of 7 × 10^{-7} meters/Volt at the high end.

A similar series of measurements on SBN:50 gave the results summarized in Table 3.1. Here one sees a steady decrease in dn_{33}/dE_3 between 33 and 37 GHz, from 5 × 10^{-7} to 1.5 × 10^{-7} meters/Volt. In view of the large sample-to-sample variability in millimeter wave dielectric properties which we have found in these materials, one should be cautious in drawing any general inferences from the trends in these data. At most, one can note that SBN:60 and SBN:50 samples showed sensitivities of the same order, closely paralleling the electro-optic

response reported for these materials. These values may be compared with the low-frequency values of $d(\sqrt{\varepsilon_{33}})/dE_3$, which for SBN:60 is about 2×10^{-6} meters/Volt at room temperature.

Table 3.1

Variations of dn/dE with Frequency and Applied Voltage for SBN:50

	$\Delta T^2(\omega)/T_o^2$	V	dn/dE
33 GHz	0.00505	65	5.054×10^{-7}
	0.00962	120	5.214×10^{-7}
	0.0171	215	5.173×10^{-7}
	0.0228	300	4.943×10^{-7}
	0.0339	400	5.513×10^{-7}
	0.0362	480	4.906×10^{-7}
	0.0472	640	4.797×10^{-7}
	0.0538	736	4.755×10^{-7}
35 GHz	0.0041	60	3.619×10^{-7}
	0.00871	120	3.844×10^{-7}
	0.0142	205	3.688×10^{-7}
	0.0228	315	3.833×10^{-7}
	0.0273	400	3.615×10^{-7}
	0.0373	512	3.858×10^{-7}
	0.0494	736	3.555×10^{-7}
37 GHz	0.00219	70	1.71×10^{-7}
	0.00459	120	2.10×10^{-7}
	0.00688	200	1.88×10^{-7}
	0.00940	350	1.47×10^{-7}
	0.0115	400	1.58×10^{-7}
	0.00757	275	1.51×10^{-7}
	0.0135	528	1.40×10^{-7}
	0.0187	736	1.39×10^{-7}

3.2 Dielectric Studies

The bulk of our dielectric measurements at millimeter wavelengths have been summarized in previous contact reports. However, the data supporting certain of our conclusions have not been presented in detail. In this section, measurements are reported on several different SBN samples, prepared under a range of conditions, and the inferences we have drawn from these data are stated

once again. Also, the results from a limited number of millimeter wave measurements on lead potassium lanthanium niobate (PKLN) ceramics are presented.

From a theoretical viewpoint the effects of poling on millimeter wave dielectric properties of SBN should be very small. To check this, two c-axis samples from the same growth were measured from 30 to 40 GHz before and after a thorough poling. One of these samples (see Table 3.2 below) turned out to have the lowest values for ε_{33} found under this program: $\varepsilon = 36 + i12$, while the other showed a more typical range around $\varepsilon = 135 + i60$. As can be seen from the Table, neither sample was much affected by the poling. Quite possibly, the details of sample fit in the waveguide are responsible for the observed differences. By far the most significant fact is the radical difference in ε between the two samples, which forces us to conclude that extrinsic factors varying during growth can swing the millimeter wave dielectric properties over a wide range. It should be noted that no comparable variations in the low frequency permittivity among poled samples has been found.

The possibility that growth striations, corresponding to small periodic fluctuations in crystal composition, could be responsible for the high observed losses was tested by annealing out all visible striations on three samples from a recent growth. Dielectric data on these samples, summarized in Table 3.3, show that losses are at least as large as in striated samples.

Minimizing the effect of impurities on the loss was attempted in growth number 112, which used ultra-pure starting materials. In this case, three samples were characterized between 90 and 100 GHz and two were measured between 30 and 40 GHz. The dielectric properties for these samples are given in Table 3.4. Once again, no significant effect on loss is seen: tan δ ranges from 0.1 to 0.7. Also, the sample-to-sample variability in dielectric properties stands out clearly, with ε' differing by a factor of two between the low-frequency samples, and by a factor of three between the two high-frequency a-axis samples.

Given this wide scatter in results, one must seriously consider the possibility that there is a hidden defect in the measurement method itself. To check the method, a high purity, high dielectric constant, single crystal of TiO_2 was obtained from Penn State and cut into appropriately dimensioned

Table 3.2

Dielectric Properties of Two SBN:60 Samples Before and After Poling

	Before			After		
F(GHz)	R^2	T^2 (x 10^{-2})	ϵ	R^2	T^2 (x 10^{-2})	ϵ
			Sample #1 Thickness = 0.874 mm			
31	0.631	2.34	35.4 + i16.3	0.625	2.51	35.5 + i15.7
32	0.631	2.75	36.7 + i14.7	0.620	2.93	36.4 + i14.2
33	0.654	3.16	38.1 + i12.8	0.622	3.18	36.1 + i13.4
34	0.661	3.30	37.6 + i12.2	0.640	3.25	36.3 + i12.8
35	0.672	3.55	37.2 + i11.1	0.654	3.38	36.2 + i12.0
36	0.678	3.89	36.3 + i10.1	0.666	3.48	35.8 + i11.4
37	0.679	4.13	35.2 + i9.5	0.669	3.72	35.0 + i10.5
38	0.683	4.49	34.2 + i8.7	0.671	3.86	34.2 + i10.0
			Sample #2 Thickness = 0.907 mm			
31	0.843	0.90	136 + i78	0.829	0.775	110 + i68
32	0.835	1.11	136 + i63	0.822	0.702	114 + i70
33	0.834	1.38	139 + i59	0.824	0.732	125 + i70
34	0.831	1.71	142 + i55	0.825	0.899	135 + i67
35	0.828	2.14	145 + i55	0.821	1.09	137 + i63
36	0.827	2.51	139 + i47	0.813	1.47	137 + i57
37	0.822	3.16	136 + i43	0.817	1.91	139 + i52
38	0.821	3.52	127 + i40	0.813	2.37	130 + i47

Table 3.3

Dielectric Properties of Three Annealed SBN:60 Samples

C-axis

	Sample #1 - Thickness = 0.376 mm			Sample #2 - Thickness = 0.419 mm		
F(GHz)	R^2	T^2 (x 10^{-3})	ε	R^2	T^2 (x 10^{-3})	ε
31	0.868	1.9	216 + i135	0.891	1.4	226 + i130
33	0.834	3.2	186 + i112	0.864	1.9	191 + i118
35	0.830	3.7	186 + i102	0.845	2.9	171 + i98
37	0.808	5.3	166 + i86	0.812	4.7	146 + i78
39	0.803	6.3	156 + i76	0.803	6.0	136 + i68

A-axis

Thickness = 0.434 mm

F (GHz)	R^2	T^2 (x 10^{-3})	ε
31	0.911	2.2	246 + i92
33	0.830	6.5	161 + i63
35	0.724	19.3	121 + i40
37	0.745	26.8	121 + i26
39	0.777	26.8	116 + i23

Table 3.4

Dielectric Properties of High Purity SBN:60 Samples

C-axis, 30 - 40 GHz

Sample #1 - Thickness = 0.480 mm				Sample #2 - Thickness = 0.475 mm		
F(GHz)	R^2	T^2 (x 10^{-3})	ϵ	R^2	T^2 (x 10^{-3})	ϵ
30	0.871	1.26	150 + i112	0.912	0.18	285 + i237
33	0.828	3.16	133 + i81	0.871	1.00	185 + i131
36	0.782	8.91	112 + i50	0.851	2.51	225 + i99
39	0.785	10.0	106 + i44	0.822	5.62	205 + i69

A-axis, 90 - 100 GHz

Sample #3 - Thickness = 0.602 mm				Sample #4 - Thickness = 0.597 mm		
92	0.871	2.00	245 + i76	0.708	6.31	65 + i17
94	0.841	2.51	215 + i72	0.776	5.62	79 + i17
96	0.822	2.24	190 + i76	0.759	5.01	75 + i18
98	0.822	2.37	190 + i73	0.759	5.01	75 + i18

C-axis, 90 - 100 GHz

Thickness = 0.457 mm

F (GHz)	R^2	T^2 (z 10^{-3})	ϵ
91	0.794	10.1	131 + i18
93	0.794	7.94	127 + i21
95	0.794	8.32	124 + i20
97	0.794	10.0	120 + i18
99	0.794	10.0	117 + i17

samples for measurement at 30 - 40 and 90 - 100 GHz. The results of the measurements are shown in Table 3.5. Values derived from the permittivity along the two principal directions show good internal consistency when samples of different thickness are used, and they are generally in agreement with low frequency data on this material. There is some indication of a decrease in the larger permittivity at 90 GHz, which may be an artifact of the method. Good sample fit in the waveguide is much more critical at short wavelengths.

Table 3.5

Summary of Measured Dielectric Properties of Single Crystal TiO_2

Sample No.	Thickness (cm)	Frequency (GHz)	ε'	Loss Tangent
		Electric Field Parallel to Crystal C-axis		
1	0.1062	34.41	152.6	0.0008
2	0.1011	36.18	151.7	0.0006
1 + 2	0.2073	35.11	153.3	0.0009
a	0.098	94.86	131.2	0.0066
		Electric Field Perpendicular to Crystal C-axis		
1	0.0991	33.85	80.49	0.0003
2	0.1052	32.08	79.58	0.0004
3	0.1047	32.22	79.67	0.0004
1 + 2 + 3	0.309	32.87	79.04	
		37.66	81.80	0.0004
a	0.105	93.70	81.62	0.0018

Our dielectric measurements on the PKLN solid solution system have been confined to two compositions that are orthorhombic (and ferroelectric) at room temperature. Ceramic samples fabricated by hot pressing were measured from 30 to 40 GHz with the microwave electric field both parallel and perpendicular to the pressing axis. Dielectric data for these samples are presented in Table 3.6. Both ε' and tan δ are found to be similar in magnitude to those seen in the poorest SBN:60. Permittivities along the pressing axis are somewhat higher than those measured perpendicular to the axis.

Table 3.6

Dielectric Properties of Orthorhombic PKLN Samples

F(GHz)	Parallel to axis - thickness = 0.93 mm R^2	T^2 (x 10^{-3})	ϵ	Perpendicular to axis - thickness = 0.91 mm R^2	T^2 (x 10^{-3})	ϵ
			$Pb_{0.7}K_{0.15}La_{0.15}Nb_2O_6$			
31	0.820	2.51	122 + i47	0.785	2.75	49 + i37
33	0.794	2.51	108 + i47	0.767	2.75	58 + i38
35	0.794	1.70	108 + i51	0.755	2.14	73 + i46
37	0.766	1.20	91 + i53	0.746	1.58	79 + i49
39	0.714	1.41	59 + i44	0.736	1.26	75 + i50
			$Pb_{0.8}K_{0.1}La_{0.1}Nb_2O_6$			
	Parallel to axis - thickness = 0.96 mm			Perpendicular to axis - thickness = 0.96 mm		
31	0.822	3.16	120 + i41	0.813	2.00	110 + i48
33	0.817	1.82	118 + i50	0.794	1.45	99 + i52
35	0.820	1.00	146 + i63	0.794	0.71	102 + i62
37	0.804	0.40	142 + i76	0.762	--	--*
39	0.794	0.32	138 + i77	0.700	--	--*

*Loss measurements indeterminate due to standing wave interference.

4.0 CONCLUSIONS

4.1 A major success of this contract effort has been development of the Czochralski growth technique for the tungsten bronze family ferroelectrics, specifically SBN:50 and SBN:60 compositions. Although SBN:50 is not a congruent melting composition in this system, our technique yields high quality crystals of 2 cm in diameter for this composition.

4.2 Low frequency dielectric properties of both compositions have been evaluated and they show low loss and high permittivity as expected. However, high frequency properties of these materials are significantly different. In particular, losses at millimeter wavelengths are very high, in excess of 20 dB/mm. Such losses would appear to rule out the device applications originally envisioned to utilize the large nonlinear dielectric response. Our measurements of this response confirms that values of dn/dE of the order 10^{-6} m/V are achieved in this solid solution system.

The current observations suggest that these losses are connected to extrinsic factors acting during crystal growth and also to the distribution of Ba^{2+} and Sr^{2+} over the two 15- and 12-fold crystallographic sites in the tungsten bronze structure. Future work should concentrate on the influence of environmental factors such as temperature and pressure both during and after crystal growth. Such conditions should also be varied systematically during high frequency measurements.

4.3 In the course of this program, a variety of other ferroelectrics have been examined in ceramic form, e.g., PLZT, PZT, PKLN, PBN, PST etc. In general, the losses are substantially higher in these ceramic materials. We believe the other ferroelectrics such as $Gd_3(MoO_4)_3$ (GMO) and $Bi_4Ti_3O_{12}$ should be tried at millimeter wave frequencies. These crystals exhibit more than one polar direction, so that large anisotropic effects can be induced in these materials.

5.0 PUBLICATIONS AND PRESENTATIONS

5.1 Publications

1. R.R. Neurgaonkar, W.K. Cory, W.W. Ho, W.F. Hall and L.E. Cross, "Tungsten-Bronze Family Crystals for Acoustical and Dielectric Applications," Ferroelectrics 38, 857, (1981).

2. W.W. Ho, W.F. Hall, R.R. Neurgaonkar, R.E. DeWames and T.C. Lim, "Microwave Dielectric Properties of $Sr_{0.61}Ba_{0.39}Nb_2O_6$ Single Crystals at 35 and 58 GHz," Ferroelectrics 38, 833, (1981).

3. R.R. Neurgaonkar, J.R. Oliver, W.K. Cory and L.E. Cross, "Structural and Dielectric Properties of the Phase $Pb_{1-2}K_xM^{3+}_xNb_2O_6$, Phase, M = La or Bi," Mat. Res. Bull. 18, 735, (1983).

5.2 Presentations

1. R.R. Neurgaonkar, W.K. Cory, W.W. Ho, W.F. Hall and L.E. Cross, "Tungsten-Bronze Family Crystals for Acoustical and Dielectric Applications," presented at the 5th Int. Meeting on Ferroelectricity, Penn State Univ., PA, August 17-21, 1981.

2. W.W. Ho, W.F. Hall, R.R. Neurgaonkar, R.E. DeWames and T.C. Lim, "Microwave Dielectric Properties of $Sr_{0.61}Ba_{0.39}Nb_2O_6$ Single Crystals at 35 and 58 GHz," presented at the 5th Int. Meeting of Ferroelectricity at Penn State Univ., PA, August 17-21, 1981.

6.0 REFERENCES

1. R.E. DeWames, W.W. Ho, W.F. Hall, R.R. Neurgaonkar, and T.C. Lim, Bull. APS 26, 303, 1981.

2. R.R. Neurgaonkar, M.H. Kalisher, T.C. Lim, E.J. Staples and K.L. Keester, Mat. Res. Bull. 15, 1235 (1980).

3. W.W. Ho, W.F. Hall, R.R. Neurgaonkar, R.E. DeWames and T.C. Lim, Ferroelectrics 38, 833 (1981).

4. R.R. Neurgaonkar, J.R. Oliver, W.K. Cory and L.E. Cross, Mat. Res. Bull. 18, 735 (1983).

5. A.A. Ballman and H. Brown, J. Cryst. Growth 1, 331 (1967).

6. R.R. Neurgaonkar, W.K. Cory, W.W. Ho, W.F. Hall and L.E. Cross, Ferroelectrics 38, 857 (1981).

7. P.L. Lenzo, E.G. Spencer and A.A. Ballman, Appl. Phys. Lett. 11, 23 (1976).

8. A.M. Glass, J. Appl. Phys. 40, 4699 (1969).

9. K. Megumi, N. Nagatsuma, Y. Kashiwada and Y. Furuhata, J. Mat. Sci. 11, 1583 (1976).

10. O.F. Dudnik, A.K. Gromov, U.B. Kravchenko, Y.L. Kopylov and G.F. Kunznetsov, Sov. Phys. Cryst. 15, 330 (1970).

11. P.B. Jamieson, S.C. Abrahams and J.L. Bernstein, J. Chem. Phys. 48, 5048 (1968).

12. G. Goodman, Am. Cer. Soc. Bull. 31, 113 (1952).

13. G. Goodman, Am. Cer. Soc. Bull. 36, 368 (1953).

14. M.H. Francombe, Acta. Cryst. 13, 131 (1960).

15. V.A. Isupov, V.I. Koiakov, Zh. Tekh. Fiz. 28, 2175 (1958).

16. E.G. Bonnikova, I.M. Larionov, N.D. Smazhevskaya and E.G. Glozman, Izv. Akad. Nauk. SSR., Ser. Fiz. 24, 1440 (1960).

17. B. Lewis and L.A. Thomas, Proc. Int'l. Conf. Solid State Phys. Electronics Telecommun., Brussel 4, Pt. 2, 883 (1960).

18. G. Goodman, Am. Ceram. Soc. Bull. 34, No. 4, Program 11 (1955); U.S. Patent 2,805,165, Sept. 3, 1975, filed April 25, 1955.

19. G. Goodman, U.S. Patent 2,729,757, June 3, 1956; filed June 29, 1951.

20. P. Baxter and N.J. Hellicar, J. Am. Ceram. Soc. 43, 578 (1960).

21. E.C. Subbarao, G. Shirane and F. Jona, Acta. Cryst. 13, 226 (1960).

22. E.C. Subbarao, J. Am. Ceram. Soc. 43, 439 (1960).

23. E.C. Subbarao and J. Hrizo, J. Am. Ceram. Soc. 45, 528 (1962).

24. E.C. Subbarao and G. Shirane, J. Chem. Phys. 32, 1846 (1960).

25. L.V. Soboleva and F.I. Dmitrieva, Inorg. Mat. 6, 1761 (1970).